The focal plane of the Simbol–X space mission

B.P.F. Dirks[a], P. Ferrando[a], U. Briel[d], O. Gevin[a], E. Kendziorra[e], P. Laurent[a], O. Limousin[a], F. Lugiez[a], J. Martignac[a], M. Authier[a], C. Chapron[f], P. Lechner[g], G. Pareschi[b], Y. Rio[a], J.P. Roques[c], P. Salin[f], L.Strüder[d]

[a] CEA/Saclay, 91191, Gif-sur-Yvette, France
[b] Osservatorio Astronomico di Brera, INAF, Via E Bianchi 46, 23807, Merate, Italy
[c] CESR, 9, Ave. du Colonel Roche, Toulouse, France
[d] Max-Planck-Institut für Extraterrestrische Physik, Giessenbachstraße, Garching, Germany
[e] IAAT, Sand 1, D-72076 Tübingen, Germany
[f] APC, 11, place Marcelin Berthelot, 75231, Paris, France
[g] PNSensor, GmbH, Munich, Germany

ABSTRACT

The Simbol–X mission, currently undergoing a joint CNES-ASI phase A, is essentially a classical X-ray telescope having an exceptional large focal length obtained by formation flying technics. One satellite houses the Wolter I optics to focus, for the first time in space, X-rays above ~ 10 keV, onto the focal plane in the second satellite. This leads to improved angular resolution and sensitivity which are two orders of magnitude better than those obtained so far with non-focusing techniques. Tailored to the 12 arcmin field of view and ~ 15 arcsec angular resolution of the optics, the $\sim 8 \times 8$ cm^2 detection area of the spectro-imager has $\sim 500 \times 500$ μm^2 pixels, and covers the full energy range of Simbol–X, from ~ 0.5 to ~ 80 keV, with a good energy resolution at both low and high energy. Its design leads to a very low residual background in order to reach the required sensitivity. The focal plane ensemble is made of two superposed spectro-imaging detectors: a DEPFET-SDD active pixel sensor on top of an array of pixelated Cd(Zn)Te crystals, surrounded by an appropriate combination of active and passive shielding. Besides the overall concept and structure of the focal plane including the anti-coincidence and shielding, this paper also emphasizes the promising results obtained with the active pixel sensors and the Cd(Zn)Te crystals combined with their custom IDeF-X ASICs.

Keywords: Simbol–X, astrophysics, formation flying, X-ray optics, CdTe, IDeF-X, DEPFET

1. INTRODUCTION

Simbol–X is a next generation hard X-ray mission proposed by an international consortium of European institutes, in response to a call-for-ideas issued by CNES for a scientific payload to be put onboard a formation flight demonstrator. After a thorough assessment study, called phase 0, Simbol–X has been selected by the CNES in autumn 2005 for a phase A study, to be jointly performed by CNES and ASI. The launch date resulting from the phase 0 study is set to mid 2013. Operating in the $\sim 0.5 - 80$ keV domain, Simbol–X will fully cover the transition from thermal to non-thermal emissions, as well as the iron line region. These are two important characteristics for the study of the highly variable accreting sources which are the prime scientific targets of the mission. To reach the required sensitivity and angular resolution, a focusing technique is used. For the first time in a space environment, photons having an energy above ~ 10 keV are focused, thanks to the emerging formation flight technology. Simbol–X is equipped with a grazing incidence Wolter I optics system, carried by a mirror spacecraft, which focuses the X-rays onto a second satellite housing the detector system. The detector spacecraft maintains its position relative to the mirror by means of an active control loop on the telescope axis. Here the formation flight technology comes in. A thorough description of the scientific objectives and the overall concept of the mission is given by Ferrando *et al.*[1–3]

Further author information: (send correspondence to B.P.F. Dirks)
B.P.F. Dirks: E-mail: bdirks@cea.fr
P. Ferrando: E-mail: philippe.ferrando@cea.fr

The design of the detector assembly will be tightly tailored to the final mission parameters that are worked out and optimized during the phase A study. At this stage, the present design takes into account the most important parameters for the mission, corresponding to the $\sim$ 20 m focal length optics. These are shown in Table 1.

Parameter	Value (and origin)
Energy range	<0.5–80 keV
Energy resolution	$\sim$130 eV @ 6 keV (Fe line)
	$\sim$1 keV @ 68 keV (^{44}Ti line)
Overall size	8×8 cm^2 (coverage of 12 arcmin of F.O.V., with 20 m focal length)
Pixel size	$\sim$500$\times$500 μm^2 (oversampling of 15 arcsec HEW PSF)
Max Count Rate	$\sim$10,000 c/s (observability of a $\sim$1 Crab flux)

Table 1. The focal plane characteristics.

The above characteristics have led to the design of a two stages focal plane system which will be described in detail in the following chapters. More information about the background simulation is given by Tenzer *et al.*[4] Developments on the optics, the stray-light and thermal shielding can be found in Pareschi *et al*,[5] Cusumano *et al.*[6] and Collura *et al*,[7] respectively.

2. CONFIGURATION

The two satellites forming the Simbol–X space mission will be launched by a Soyuz rocket with a Fregat upper stage. Both vehicles will be injected in a high elliptical orbit to minimize the radiation level. The phase 0 study orbit has a perigee of 44,000 km and an apogee of 253,000 km at launch. In observation mode, the relatively heavy mirror satellite (master) maintains its orbit while the detector satellite (slave) is positioned along the mirror axis, keeping the distance between the mirror and the focal assembly at the focal length value. Fig. 1.a shows the space vessels in nominal observation mode. The baffle around the mirror and the collimator mounted on the detector satellite are a part of the radiation shielding which is explained in detail in Chapter 5. Since this paper is dedicated to the focal plane only, we will focus on the detector vehicle which is detailed in Fig. 1.b-f. It consists of a focal plane detection area with a low and high energy detector surrounded by an active and passive shielding inside a protective aluminium enclosure. Located on the top are a turnable disk, which offers the possibility to operate in calibration, protection and measurement mode, and the collimator to stop diffuse background photons. The thermal lines to the detectors are linked to an external radiator by means of a heat-pipe to allow passive temperature control. The operating temperature will be between -30 and -40^{o}C.
Surrounded by an active and passive shielding are the silicon low energy detector (Chapter 3) on top of the Cd(Zn)Te* high energy detector (Chapter 4). The former is built from a single silicon wafer which is divided into four regions which can be read out independently while the Cd(Zn)Te detector is constructed from 8 identical modules of 2×4 individual X-ray cameras (Fig. 1.e-f). An individual camera is a hybridization of a 2 mm thick Cd(Zn)Te crystal covered with 256 pixels of 500 μm^2 surrounded by a guard ring and an IDeF-X ASIC. The modular design has the advantage that the different modules can be tested and replaced separately.

3. THE LOW ENERGY DETECTOR

The low energy detector (LED) of Simbol–X is a silicon drift detector (SDD) with DEPFET (DEPleted Field Effect Transistor) readout (see Fig. 2), also called "Macro Pixel Detector" or "Active Pixel Sensor" (APS). Prototypes of macro pixel detectors have already been developed, built and tested by the MPI semiconductor laboratory (HLL)[8–10] . The LED consists of 128×128 pixels with a baseline size of 500×500 μm^2 with $\sim$450 μm depletion depth. This thick depleted bulk in combination with a thin entrance window results in a high quantum efficiency of the bare detector of already >85% at 100 eV, 95% at 10 keV and still 45% at 20 keV. However, the thermal blanket in front of the mirrors and the optical filter of the detector will limit the lower energy of the LED to 0.5 keV, resulting in a nominal energy range for the LED of $\sim 0.5 - 20$ keV. The detector

*Cd(Zn)Te standing for CdTe or CdZnTe. The final material choice will be made at the end of phase A.

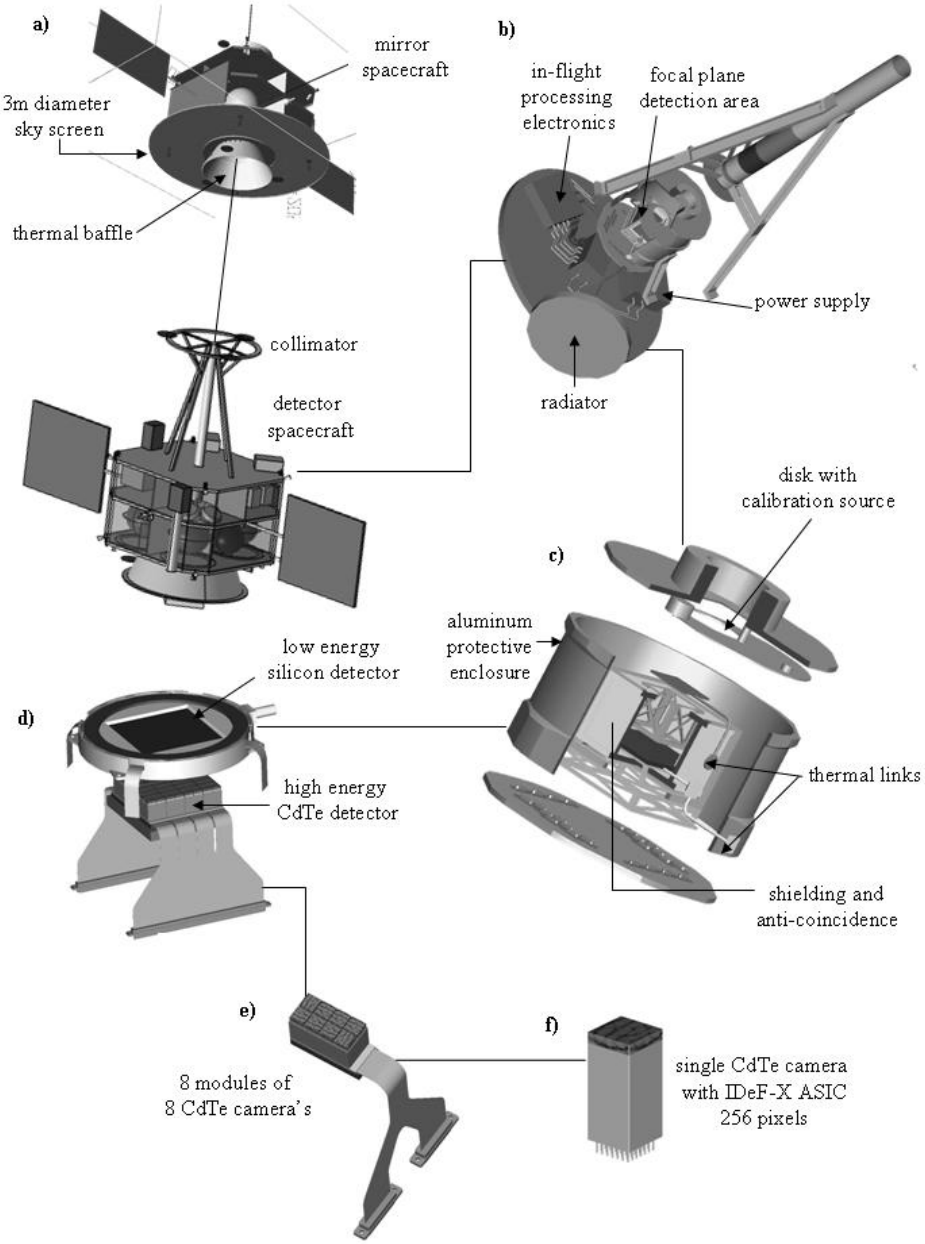

Figure 1. The Simbol–X mission configuration: a) In observation mode the detector satellite will follow the mirror satellite on a high elliptical orbit. The sky screen and collimator prevent background photons to enter directly the opening in the detector satellite. b) The focal plane, with the detection area, electronics, power supply, radiator etc. c) The detection area is protected by an aluminium enclosure which contains an active and passive shielding surrounding the low and high energy detectors (Si and Cd(Zn)Te resp, displayed in d.) The thermal links and large radiator allow temperature controlling. e) The Cd(Zn)Te detector is built from 8 identical modules of 2×4 X-ray cameras. f) An individual camera is a hybridization of a Cd(Zn)Te crystal having 256 pixels connected to the IDeF-X ASIC.

is logically and functionally divided into four quadrants of 64×64 pixels each. All four quadrants are read out in parallel at a frame time of 256 μs. This short integration time allows the operation of the detector even at room temperatures with an expected energy resolution of about 500 eV (FWHM). In order to further reduce the noise contribution by leakage currents and to achieve an energy resolution of <145 eV (FWHM) at 5.9 keV, the wafer must be cooled down to only -30^{o}C (assuming a leakage current of 0.26 nA/cm^2 at room temperature). We note however, that the energy resolution strongly depends on the pixel size (and the frame time). Increasing the pixel size requires a lower operation temperature.

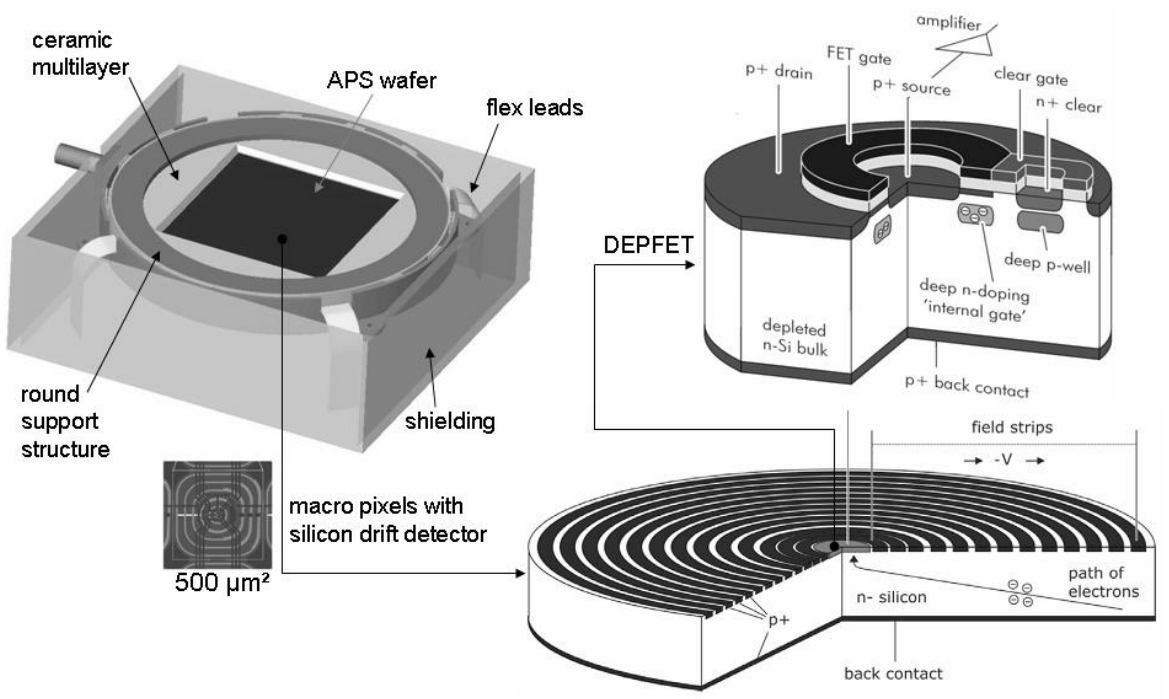

Figure 2. Present concept of the Simbol–X low energy detector formed by a single silicon wafer with 128 by 128 pixels which is logically divided into four quadrants of 64×64 active pixel sensors, consisting of a silicon drift detector with DEPFET read-out. The wafer is mounted between two ceramic boards which themselves are clamped by the round support structure. The baseline pixel size is envisaged to be a square of 500×500 μm^2.

3.1. Mechanical concept of the low energy detector

The left part of Fig. 2 (see also Fig. 1) shows the present mechanical concept of the low energy detector inside the detector spacecraft. The central square represents the area of the active pixel sensor (APS) with its 128×128 pixels, which are integrated onto one single silicon wafer. The wafer is mounted between two ceramic boards which themselves are clamped by the round support structure. The support structure has an interface to a heat pipe which is connected to the radiator. The passive cooling, together with active heaters, will allow stabilizing the operating temperature of the silicon wafer. Since the APS is backside illuminated, the (not visible) lower ceramic board is designed as a multi-layer board and will contain the front-end electronics of the APS such as the CAMEX readout ASICs and the SWITCHER control ASICs. The latter are connected to the rows and channels of the APS via wire bonds. Indicated in the corner are flex-leads which connect the front-end electronics with the sequencer electronics, ADCs and digital electronics, and with the power supplies. The entrance window of the detector will be coated by a thin aluminium layer, which will suppress optical light. The APS support structure is surrounded by the anti-coincidence and shielding system (see Chapter 5).

3.2. Electrical concept

Fig. 3 shows the silicon wafer divided into four quadrants of 64×64 macro-pixels of 500 μm^2 (pointed out). On the right is the electrical block diagram of the assembly. Each quadrant of the LED has its own power supply unit and readout electronics. In full frame mode the 4096 pixels of a quadrant are read row by row, the active row being selected by the gate SWITCHER and reset by the clear SWITCHER. All other pixels are turned off and are in integration mode until they are activated for read out. The 64 pixels of an active row are processed in parallel by a preamplifier filter and multiplexer chip, called CAMEX64, which is an improved version of the CAMEX successfully operating in the EPIC pn-CCD camera on board of XMM-Newton since more than 6 years. After signal sampling, the internal gates of the 64 active DEPFETs are cleared by a short (∼200 ns) clear pulse from the clear switch chip. After the clear process, the pixel output returns to its reference level. This level is probed by baseline samplings. The difference between signal and baseline is then stored in an analogue shift register for serial readout while the 64 pixels from the next row are processed. Our aim is to read out one row within 4 μs, resulting in a total read-out time for the full frame mode of only 256 μs. The output of the CAMEX is then converted by a fast 12 bit ADC and the pixel information from one frame is further processed by the digital event pre-processor.

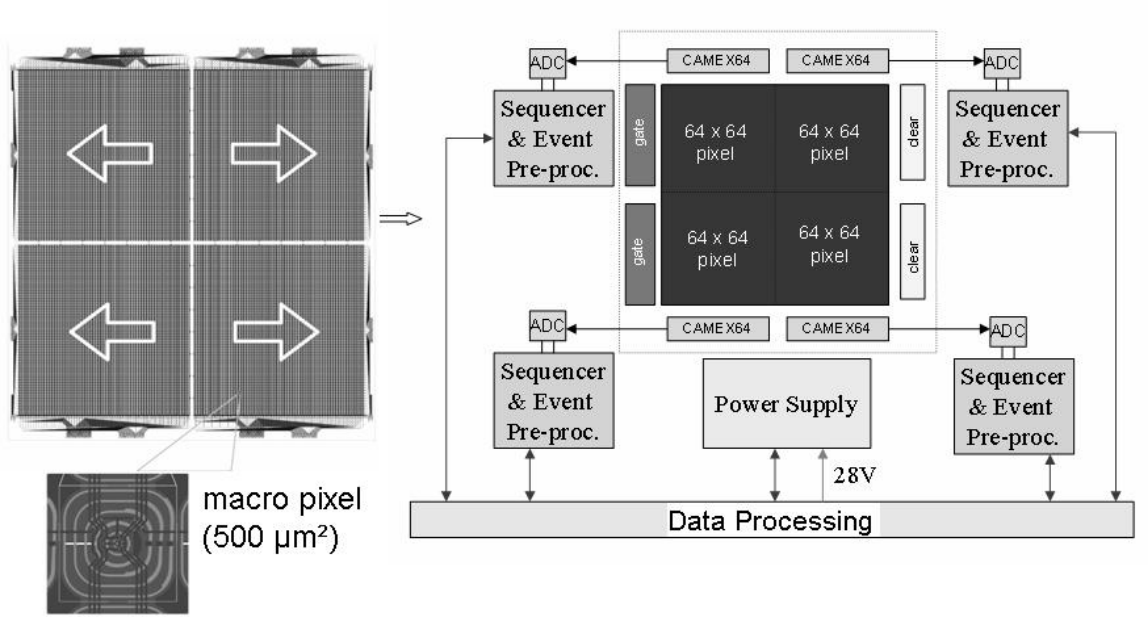

Figure 3. The silicon wafer is logically divided into four blocks of 64×64 macro pixels. On the right, we show the electrical block diagram of the low energy detector assembly.

4. THE HIGH ENERGY SPECTRO-IMAGER

The high energy detector (HED) of Simbol–X will be constructed from 4-side juxtaposable pixelated CdTe or CdZnTe crystals ($10 \times 10 \times 2$ mm^3) covered with 256 pixels of about 500×500 μm^2 in size. Both material types are studied at the moment. Each crystal is connected to its own read-out electronics, the IDeF-X (Imaging Detector Front-end for X-rays) ASIC[11] developed by CEA/Saclay, forming a complete individual X-ray camera which allows operating in the 5–100 keV range partly overlapping the low-energy range of the silicon detector. In the current design eight individual X-ray camera's will be merged to form a 2-by-4 module having its own flex for in- and output signals. The detection plane will be covered with eight of such modules. To fulfil the scientific demands of the mission, a high energy resolution of ∼1 keV at 60 keV is required for a pixel size of $\sim 500 \times 500$ μm^2 (see table 1). Reliable, radiation tolerant, low power consuming and low-noise read-out electronics in combination with high quality Cd(Zn)Te crystals covered with small pixels are therefore mandatory.

4.1. IDeF-X v1.0 ASIC

The IDeF-X v1.0 ASIC is one of the prototype designs in the development of the final complex multi-channel circuit for high density pixel detectors, such as the 256 pixels Cd(Zn)Te detector for Simbol–X, but also for the coded aperture telescope ECLAIRs.[12] Presently we report on the latest version of the IDeF-X ASIC in combination with several pixelated CdZnTe and single pixel CdTe Schottky detectors.
The full custom ASIC has been manufactured using the AMS 0.35 μm CMOS technology. Each of the 16 analogue channels of the prototype is designed to be DC coupled to detectors having a low dark current (1 pA to 1 nA per pixel) and is optimized for input capacitances ranging from 2 to 5 pF. A channel consists of a charge sensitive preamplifier, a pole zero cancellation stage, a variable peaking time filter and an output buffer. Table 2 shows a summary of its main characteristics. The next prototype (v1.1) will also be equipped with a discriminator, a peak detector and a multiplexed analogue output.

PARAMETER	VALUE
CHIP SIZE	2355 µm × 4040 µm
NUMBER OF CHANNELS	16
POWER SUPPLY	3.3V
POWER DISSIPATED	2.26 mW/channel
GAIN	200mV/fC at 6µs peaking time
DYNAMIC RANGE	-40000 to 40000 e^- (0 to 176 keV for CdTe)
SHAPING TYPE	Unipolar
PEAKING TIMES (IN µs)	0.5 / 0.9 / 1.5 / 2.4 / 3 / 4 / 4.5 / 6

Table 2. IDeF-X V.1.0. characteristics.

Its use in space applications implies a thorough study of the radiation hardness of the electronics. We therefore irradiate bare IDeF-X chips at a dose rate of 0.5 krad/h using a ^{60}Co source to simulate the space environment to which they will be exposed during the Simbol–X mission. As a controlling parameter we use the electronics noise of the chip. Before irradiation a 32 electrons equivalent noise charge (ENC) has been measured. After 40 hours, or 20 krad of total absorbed dose equivalent to the expected total dose during the mission, an ENC of 35 electrons is measured. Even after 200 hours, or 100 krad, the noise remains below 50 electrons. The cumulative dose effect shows no significant consequences for the functioning and performance of the electronics. The next step is to study transient effects induced by cosmic rays. The single event latch-up (SEL) sensitivity, using heavy ions, will be measured soon. The single event upset (SEU) sensitivity will be measured on an advanced design including more digital electronic components.

4.2. Pixelated CdZnTe and single pixel CdTe Schottky detectors

The excellent performances of the CdTe polycells in the INTEGRAL gamma-ray camera ISGRI[13] have led to the choice of the use of CdTe or CdZnTe crystals as detection material in the high-energy detector of Simbol–X. CdZnTe differs slightly from CdTe. The addition of a Zn component leads to a larger bandgap which favors a low leakage current, even at room temperature. Also, the electron mobility is higher than in CdTe. However despite its smaller bandgap, CdTe allows using Schottky contacts which also leads to smaller leakage currents. Both materials types have their proper advantages and disadvantages that will be studied in detail in phase A. In the approach to the final 256 pixels (0.5×0.5 mm^2) Cd(Zn)Te X-ray camera, we study prototype 64 pixels $Cd_{0.9}Zn_{0.1}Te$ detectors (eV-products, USA). The crystals are $10 \times 10 \times 2$ mm^3 in size and are covered with 64 platinum pixels of 0.9×0.9 mm^2 surrounded by a 0.9 mm large guard ring on one side and a platinum planar

electrode on the other side. We also use single pixel CdTe detectors (ACRORAD, Japan) of $4.1 \times 4.1 \times 0.5$ mm^3 in size, having a platinum pixel of 2×2 mm^2 surrounded by a 1 mm large guard ring. The planar side is equipped with an indium electrode having a low work function favoring a relatively large Schottky barrier. This leads to small dark currents even at room temperature and high bias voltages (<10 pA at 4 kV/cm). Since the value of these currents can be compared with the dark current per pixel in the pixelated detectors, which are of the order of ∼100 fA at -12^{o}C, 250V, up to ∼100 pA at 20^{o}C, 500V (see Dirks *et al.*[14]), single pixel CdTe detectors are used to test individual channels of the ASICs.

4.3. Results

Fig. 4 shows the top view of a single pixel CdTe detector in its aluminium housing mounted on a teflon plate. The pixel is connected to a channel of the IDeF-X ASIC by an enamel wire. The ASIC board is fabricated from teflon glass to reduce noise from dielectric losses and capacitive load. The ASIC plus board are installed on a polarization board of standard epoxy material which is used for biasing, configuration, injection and response measurements of the electronics and detector. The CdTe crystal is biased at 330 V and irradiated from the pixel side with an ^{241}Am source. Thanks to the extremely low noise IDeF-X electronics and low dark current in the CdTe an excellent resolution is obtained of 1 keV (FWHM) at 60 keV and 735 eV (FWHM) at 13.9 keV, 22^{o}C.

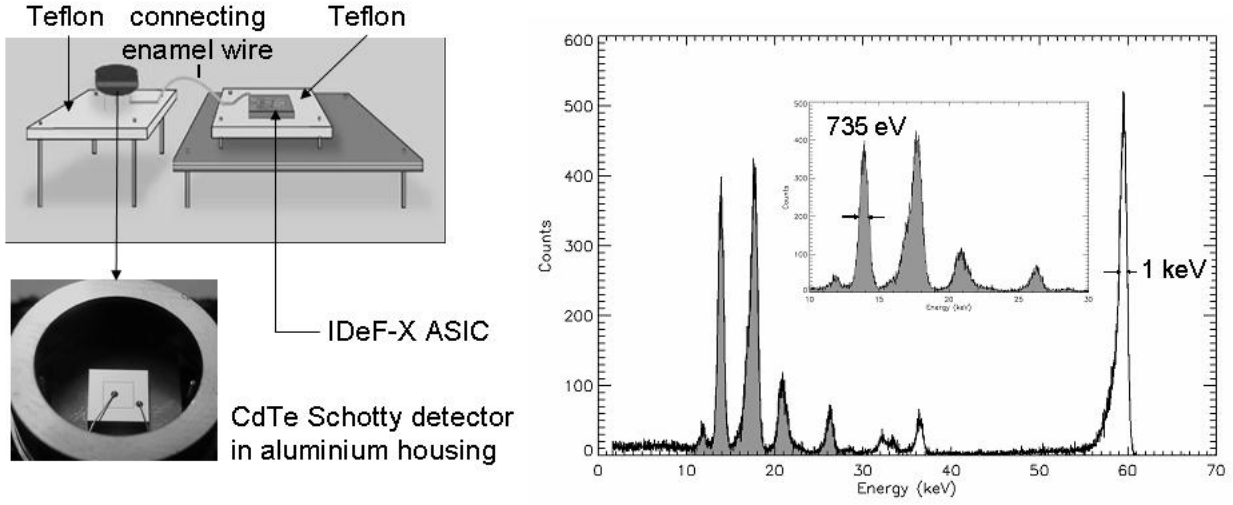

Figure 4. Measurement setup used to obtain the spectrum of an ^{241}Am source with a $4.1 \times 4.1 \times 0.5$ mm^3 CdTe detector equipped with an indium Schottky contact at the anode. The cathode is a 2×2 mm^2 platinum pixel surrounded by a 1 mm large guard ring. The detector is polarized at 330 V at a temperature of 22^{o}C. The single pixel is connected to channel 8 of the IDeF-X V1.0 ASIC by an enamel wire. The peaking time is set at 6 μs. The best spectrum is obtained at the highest peaking time because of the very low leakage current of the detector. Detector and ASIC are mounted on Teflon boards to avoid excessive noise.

In parallel to the Cd(Zn)Te crystals and electronics characterization a detailed detector modelling and electronics simulation is performed. We use the combined forces of GEANT4, to simulate particle interaction inside the bulk Cd(Zn)Te, and a Matlab program, MGS-CdTe V1.0, based on MGS.[15] The latter allows modelling of the detector geometry, electrical field and charge carrier transport, including trapping effects. It simulates the induced currents on the pixels caused by moving charge carriers created by the incoming photons. By convoluting these currents with the (numerical) impulse response function of IDeF-X V1.0, a complete detector response is generated. The simulation chain serves as a powerful tool to study signal shape, cross-talk between pixels and read-out strategy. Fig. 5.a shows the comparison between a simulated (dotted) and measured (solid, filled) ^{241}Am spectrum using a single pixel CdTe Schottky detector biased at 350 V at room temperature, with an equivalent noise charge of 66 e$^-$. The polarization effect inside the detector, caused by charge accumulation near the Schottky barrier, is not implemented yet, neither some small energy lines in the measured spectrum.

In spite of this, the correspondance is rather good. Furthermore, Fig. 5.b shows the simulated energy resolution (FWHM) as function of the ENC at four different energies. The measured result at 59.54 keV, 66 e^- ENC, has been emphasized. These graphs make it possible to predict the energy resolution as a function of the noise which is related to the dark and leakage current inside the detector and therefore directly related to the temperature and applied voltage.

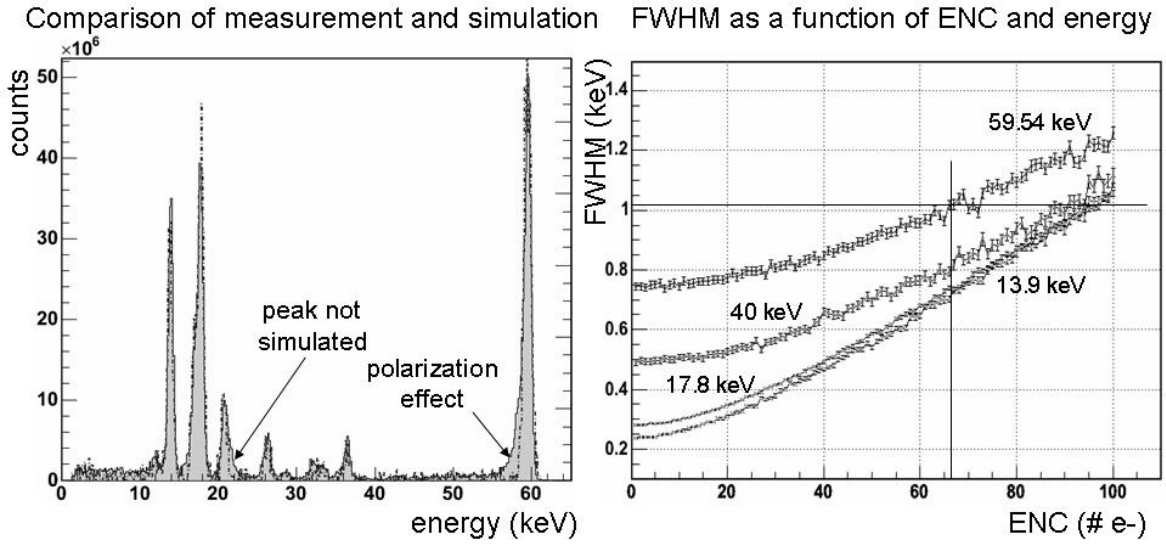

Figure 5. a) Comparison between the measured (solid) and simulated (dotted) spectrum of ^{241}Am using a single pixel CdTe Schottky detector biased at 350 V at room temperature, in case of an equivalent noise charge of 66 e^-. The polarization effect is not implemented yet, neither some small energy lines present in the measured spectrum. b) The simulated energy resolution (FWHM) as a function of the equivalent noise charge (ENC) at four different energies.

Fig. 6 shows the experimental setup used to take spectra from pixelated CdZnTe detectors. Four IDeF-X V.1.0 ASICs serve to read-out the 64 pixels of the crystal, each pixel connected to an individual input channel. The electronics and detector are mounted onto a copper plate which can be thermally controlled. The whole system is installed in a large, grounded test-chamber which allows controlling humidity and serves as an electromagnetic shield. The output signals are sent to several ADCs outside the chamber and are read out by a standard multi-channel analyzer. We show the result for one pixel but the others show comparable spectra (with a few exceptions aside). A resolution of 1.48 keV (FWHM) at 59.54 keV and 1.33 keV (FWHM) at 13.9 keV is obtained at a temperature of -11^o and a bias voltage of 500 V.

We also studied the detector behavior as a function of the temperature. Fig. 7 shows the resolution in FWHM at 59.54 keV for several pixels. They follow a nice descending trend until -10^{o}C. From there the average resolution stays constant at a value of $\sim$1.5 keV. This is most probably due to noise created by dielectric losses and capacitive load of the different interconnections and materials used in the setup. For example, the CdZnTe crystal is mounted onto a standard epoxy board which is a significant source of noise which becomes dominant at these low temperatures. If we would follow the trend, by ignoring the plateau, we should be able to reach the required resolution for Simbol–X (1 keV at 60 keV) at a temperature of about -40^{o}C.

An important step in the development of the high energy camera, is the hybridization of the pixelated crystals with the IDeF-X ASICs. Major progress has been made in this field and we will therefore be able to present a completely functional prototype X-ray camera (64 pixels) in a forthcoming paper.

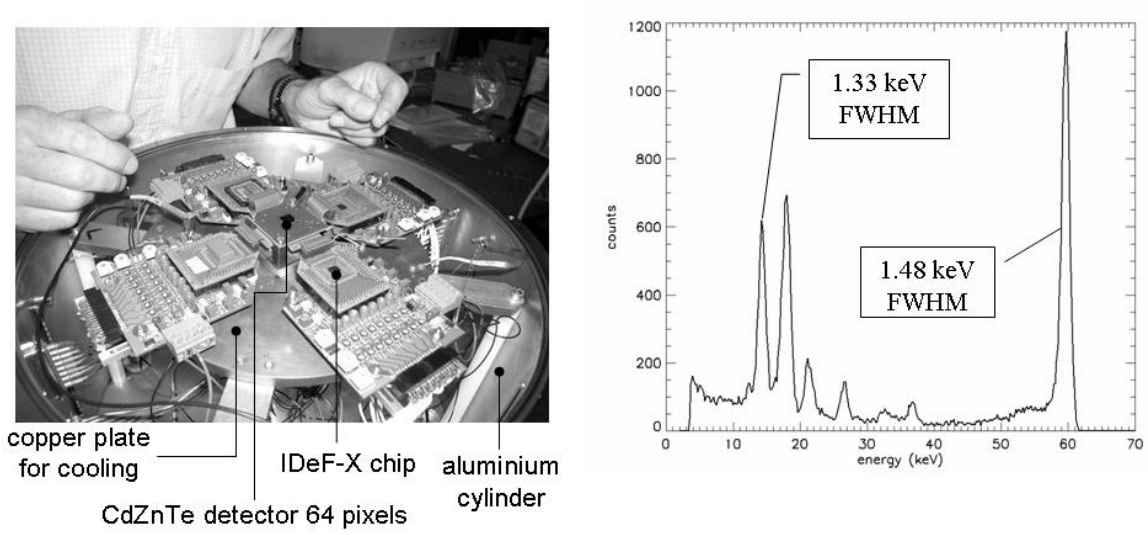

Figure 6. A CdZnTe detector of $10 \times 10 \times 2$ mm^3 covered with 64 platinum pixels of 0.9×0.9 mm^2, surrounded by a 0.9 mm large guard ring, connected to four IDeF-X V.1.0 ASICs. The spectrum on the right is taken from one of the pixels. A resolution of 1.48 keV at 59.54 keV and 1.33 keV at 13.9 keV is obtained at a temperature of -11^{o}C and a bias voltage of 500 V.

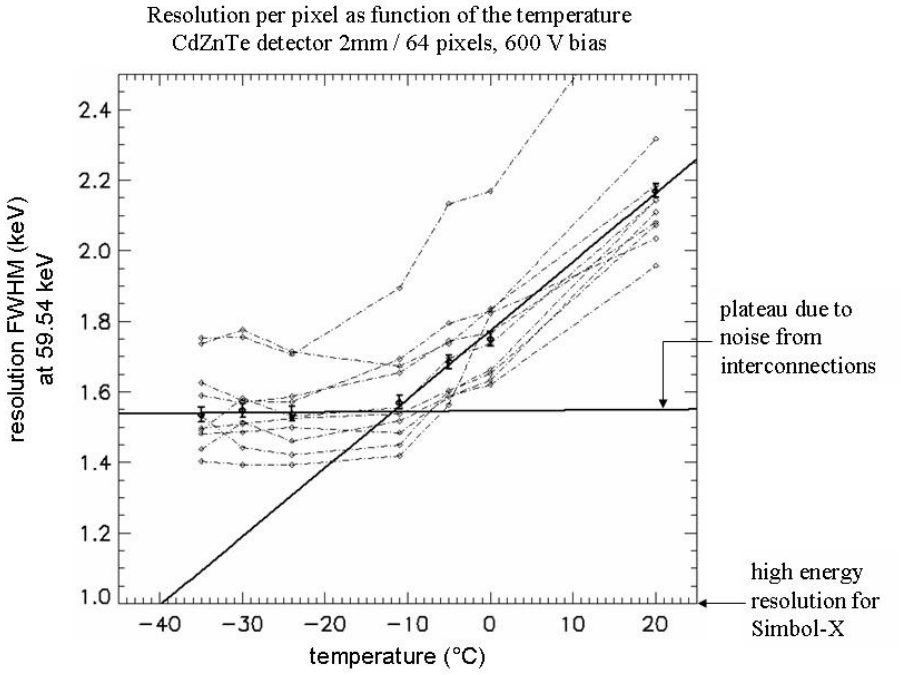

Figure 7. The resolution (FWHM) at 59.54 keV as a function of the temperature for several pixels of a 64 pixels CdZnTe detector biased at 600 V. At temperatures below -10°C the resolutions stays at a constant value of $\sim$1.5 keV. This is probably due to the noise created by the different interconnections and materials in the setup. The required resolution of 1 keV at 60 keV for Simbol–X is reached at -40°C if we would follow the trend-line.

5. SHIELDING

Since the mission consists of two satellites without any telescope tube connecting them, diffuse background photons, not coming from the mirror, can directly enter the detector spacecraft through its aperture, decreasing the sensitivity. The problem is resolved by putting a baffle around the mirror spacecraft that screens a large part of the sky without interfering the mirror's field of view. In addition a collimator is placed on the opening of the detector spacecraft (see Fig. 8). Both elements are composed of a layer of tantalum (with a transmission coefficient of $\sim 10^{-4}$) followed by a series of layers of different materials, each able to stop the fluorescence photons of the previous layer although emitting a lower energy X-ray. In the present configuration this multi-layer is fabricated from Ta (tantalum), Sn (tin), Cu (copper), Al (aluminium) and C (carbon). The latter will emit photons of $\sim$0.4 keV which are below the low energy threshold level of Simbol–X.

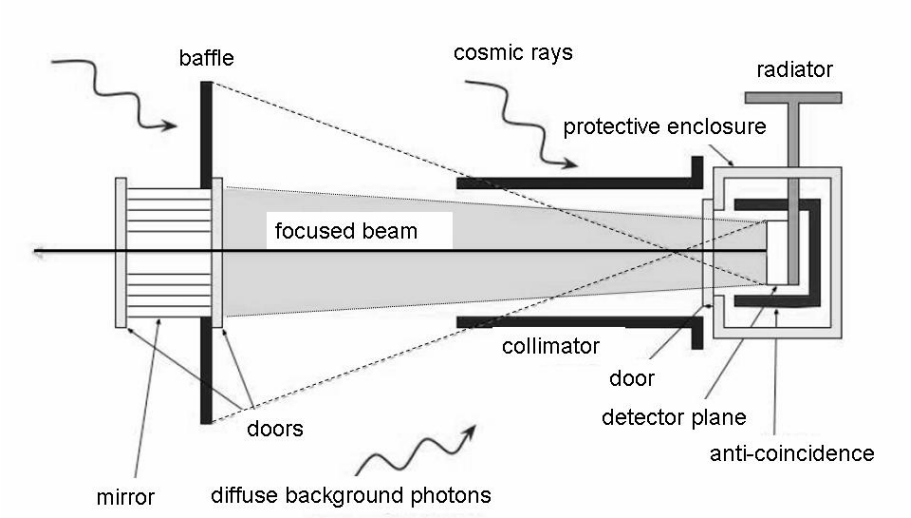

Figure 8. To avoid diffuse background photons entering the detector spacecraft by its aperture, a baffle is installed around the mirror to screen a part of the sky. In addition a collimator is placed directly on top of the opening to the detector plane. An anti-coincidence and passive shielding around the detectors serve to detect and stop cosmic rays (especially protons) hitting the spacecraft.

Beside the X-rays entering the detector housing directly, we also need to take account for the cosmic rays (essentially protons) hitting the detector spacecraft isotropically, inducing a high detection count rate. We will use an active anti-coincidence (AC) system in combination with a passive shielding. When a proton crosses the payload, it triggers simultaneously the detectors and the active shielding. The recorded event is tagged and can be easily removed from the science data. Prompt secondary particles generated by incoming cosmic-rays can also be removed by this means. Presently we are studying two possible shielding configurations: the first consists of plastic scintillators in combination with a passive shielding of the same material as the collimator. The second configuration is constructed from NaI crystals only. The former has the advantage that it is mechanically and electronically easy to construct (small photodiodes are used for the scintillator read-out) and uses no high voltage (HV). Photons with energies <100 keV are stopped and protons can be detected. However, photons having an energy superior to 100 keV can easily traverse the shield. In the case of NaI, γ <100 keV are stopped. In addition, protons and γ >100 keV are detected. Analysis and simulation work is currently being performed to optimize the choice between these two options.

Fig. 9 shows a detailed view of the detection area with the different anti-coincidence layers and shielding as foreseen in the configuration using scintillators. The two detectors are protected by a first, exterior shielding surrounding the whole system except for the X-ray entrance aperture and the opening for the different flexes and thermal links. To avoid particles entering via the latter opening, a second, inner shielding is added. In this

setup, a veto count rate of about 5000 cts/s is expected. A veto window of 1μs is foreseen to guarantee that the dead time generated by the veto signal stays well below 1 %. This requires a measurement of the signal time with an accuracy of about 10 % of the coincidence window size, i.e. 100 ns.
A detailed description of the approach to the presented shielding configuration is given by Malaguti *et al.*[16]

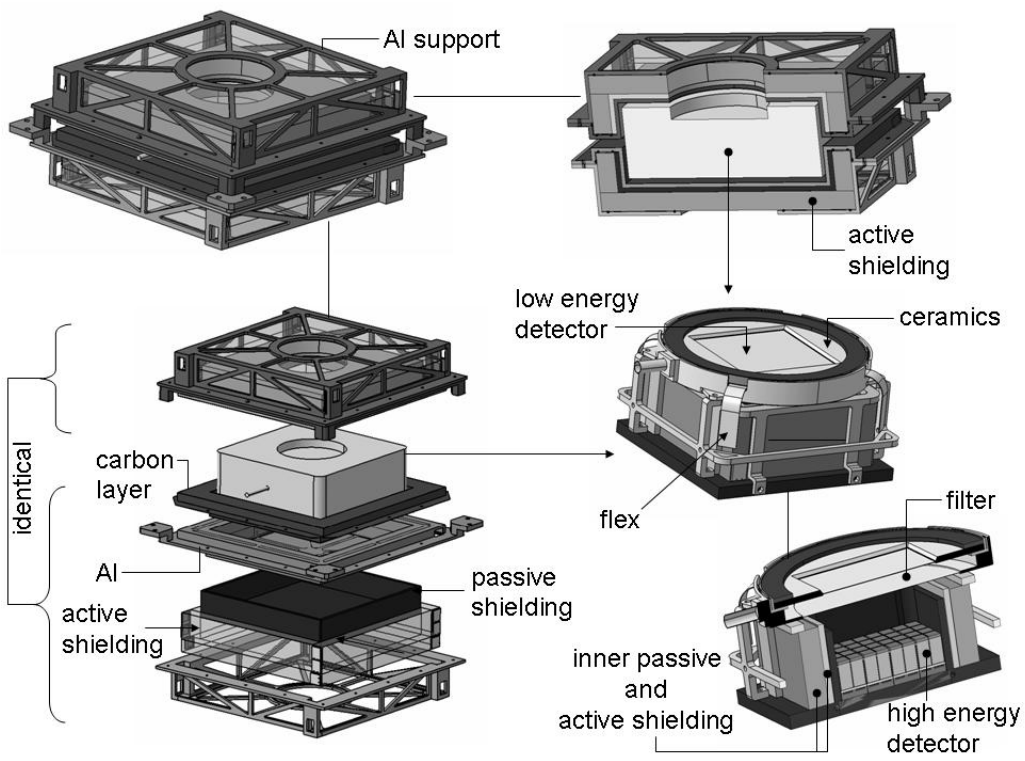

Figure 9. Exploded view of the Simbol–X focal plane, showing the arrangement of the different layers of the AC/shielding system.

6. CONCLUSIONS

We have presented the main characteristics and development status of the focal plane assembly for the Simbol–X mission. These are in line with the most demanding requirements envisioned at the beginning of phase A. No serious obstacles have been identified and promising results have already been obtained with prototypes of the two spectro-imaging detectors. We emphasized the shielding and anti-coincidence system that minimizes the residual background, originating from X–rays outside the field-of-view, and from particle interactions inside the detector surroundings.

ACKNOWLEDGMENTS

The authors would like to thank the people of CNES for their constant help in the research and development program on the Cd(Zn)Te pixelated detectors. Also, this work could not have been done without the important input and devotion of the technical and engineering staff of CEA/DAPNIA, which is warmly acknowledged here.

REFERENCES

1. P. Ferrando *et al.*, "SIMBOL-X, a new generation hard X-ray telescope," *Proc. SPIE* **5168**, pp. 65–76, 2004.
2. P. Ferrando *et al.*, "SIMBOL-X: a formation flying mission for hard-x-ray astrophysics," *Proc. SPIE* **5900**, pp. 195–204, 2005.
3. P. Ferrando *et al.*, "SIMBOL-X: mission overview," *Proc. SPIE* **6266-17**, 2006.
4. C. Tenzer *et al.*, "MC simulations of stacked SDD/CdZnTe X-ray detector arrays as designed for SIMBOL-X," *Proc. SPIE* **6266-97**, 2006.
5. G. Pareschi *et al.*, "Scientific payload for SIMBOL-X," *Proc. SPIE* **6266-92**, 2006.
6. G. Cusumano *et al.*, "SIMBOL-X: stray-light analysis and engineering solutions," *Proc. SPIE* **6266-58**, 2006.
7. A. Collura *et al.*, "Thermal shielding of SIMBOL-X X-ray telescope," *Proc. SPIE* **6266-150**, 2006.
8. J. Treis *et al.*, "Noise and spectroscopic performance of DEPMOSFET matrix devices of XEUS," *Proc. SPIE* **5898**, pp. 256–266, 2005.
9. J. Treis *et al.*, "Advancements in DEPMOSFET device developments for XEUS," *Proc. SPIE* **6276-17**, 2006.
10. L. Strüder *et al.*, "Active X-ray pixel sensors with scalable pixel sizes from 1 μm^2 to 10^8 μm^2 in Heaven and on Earth," *Proc. SPIE* **6276-48**, 2006.
11. O. Gevin, *et al.*, "IDeF-X V1.0: a new sixteen-channel low noise analogue front-end for Cd(Zn)Te detectors," *4th International Conference On New Developments in Photodetection, Beaune, to be published in NIM-A* , 2005.
12. S. Schanne *et al.*, "The space borne multi-wave-length gamma-ray burst detector ECLAIRs," *Proc. IEEE NSS-MIC*, 2004.
13. F. Lebrun, "The ISGRI CdTe gamma camera in-flight performance," *IEEE Transactions on Nuclear Science* **52-6**, 2005.
14. B.P.F. Dirks, *et al.*, "Leakage current measurements on pixelated CdZnTe detectors," *4th International Conference On New Developments in Photodetection, Beaune, to be published in NIM-A* , 2005.
15. C. S. P. Medina and D. Villaum, "A simple method for the characterisation of HPGe detectors," *Instrumentation and Measurement Technology Conference*, 2004.
16. G. Malaguti *et al.*, "Active and passive shielding design optimization and technical solutions for deep sensitivity hard X-ray focusing telescopes," in *Optics for EUV, X-Ray, and Gamma-Ray Astronomy II*, *Proc. SPIE* **5900**, pp. 159–171, 2005.